depends on the polarized remodelling of cell junctions. Junctions are remodelled through the polarized recruitment of myosin II within the plane of the epithelium. The contractile activity of myosin II might create a local tension that orients the disassembly of E-cadherin junctions. Alternatively, myosin II might interact with and control the activity of regulators of E-cadherin stabilization. Myosin II is required to progress from the type 1 to the type 2 configuration, counteracting the effect of junction formation and stabilization present at all cell junctions in epithelial cells before and during GBE. In principle, when cell–cell contacts are in the type 2 configuration, new contacts would form either by reverting to the type 1 configuration or by progressing to the type 3 configuration. However, we propose that the polarized localization of myosin II counteracts attempts to form new type 1 junctions, thus allowing the formation of only type 3 junctions. In other words, the polarized localization of myosin II determines the irreversible transformation from type 1 to type 3. This basic cellular mechanism could be involved in a variety of biological contexts in different organisms. Epithelial tubes, for instance, elongate during organogenesis from *Drosophila* to vertebrates[2,27,28]. Nevertheless, the mechanisms that orient the polarized recruitment of myosin might vary. During GBE, local signalling between adjacent cells along the A/P axis might suffice to recruit myosin II along A/P junctions specifically. In other contexts, long-range signalling by the Frizzled/Dishevelled planar cell polarity pathway might be involved[1,29]. The work presented focuses on the cellular effectors of such signalling pathways and shows how they might underlie a variety of morphogenetic processes. □

Methods

Imaging techniques

Confocal time-lapse images were collected using a spinning-disc confocal head (Perkin Elmer) run by Metamorph software on an inverted microscope (Zeiss). Phase-contrast time-lapse images were collected on an inverted microscope (Zeiss) and a programmable motorized stage to record different positions over time (Mark&Find module from Zeiss). The system was run with AxioVision software (Zeiss) and allowed the acquisition of large time-lapse data sets in mutant or injected embryos.

RNA interference

dsRNA probes to *Krüppel* (between positions 494 and 1268 of the coding sequence) and *fog* (860 bases, −24 from 5′ of the ATG to position 837 3′ of the ATG) were synthesized *in vitro* and injected in early embryos (less than 1 h old) at 0.5 $\mu g\,\mu l^{-1}$.

Injections

Y-27632 was prepared as a 50 mM stock in water and injected at 600 μM at the onset of cellularization. The dilution factor of Y-27632 in the syncytial embryo was estimated to be 1:50, so we estimate the local concentration as about 12 μM.

Genetics

The following stocks were used. *ubi-E-cad*–GFP homozygous flies (chromosome II) express a functional E-cadherin–GFP fusion[8]. The functional Sqh–GFP fusion was expressed with a genomic rescue transgene in a *sqhAX3*-null mutant background[26]. The following stocks were used to assess the role of myosin II in Fig. 3: *cn bw sp. zip*^{2}/*Cyo*, *c wt zip*^{1}/*Cyo*, *EcadGFP sp. zip*^{2}/*Cyo* and *y w sqhAX3/FM7*. The ectopic expression of a *UAS-SlamHA* transgene during GBE was monitored in embryos laid by *matαtub-Gal4VP16* mothers crossed to *UAS-slamHA* males.

Received 27 February; accepted 23 April 2004; doi:10.1038/nature02590.

1. Wallingford, J. B., Fraser, S. E. & Harland, R. M. Convergent extension: the molecular control of polarized cell movement during embryonic development. *Dev. Cell* **2,** 695–706 (2002).
2. Keller, R. Shaping the vertebrate body plan by polarized embryonic cell movements. *Science* **298,** 1950–1954 (2002).
3. Irvine, K. D. & Wieschaus, E. Cell intercalation during *Drosophila* germband extension and its regulation by pair-rule segmentation genes. *Development* **120,** 827–841 (1994).
4. Lecuit, T. & Wieschaus, E. Junctions as organizing centers in epithelial cells? A fly perspective. *Traffic* **3,** 92–97 (2002).
5. Knust, E. & Bossinger, O. Composition and formation of intercellular junctions in epithelial cells. *Science* **298,** 1955–1959 (2002).
6. Nelson, W. J. Adaptation of core mechanisms to generate cell polarity. *Nature* **422,** 766–774 (2003).
7. Adams, C. L. & Nelson, W. J. Cytomechanics of cadherin-mediated cell–cell adhesion. *Curr. Opin. Cell Biol.* **10,** 572–577 (1998).
8. Oda, H. & Tsukita, S. Real-time imaging of cell–cell adherens junctions reveals that *Drosophila* mesoderm invagination begins with two phases of apical constriction of cells. *J. Cell Sci.* **114,** 493–501 (2001).
9. Rivera-Pomar, R. & Jackle, H. From gradients to stripes in *Drosophila* embryogenesis: filling in the gaps. *Trends Genet.* **12,** 478–483 (1996).
10. Small, S., Kraut, R., Hoey, T., Warrior, R. & Levine, M. Transcriptional regulation of a pair-rule stripe in *Drosophila*. *Genes Dev.* **5,** 827–839 (1991).
11. Costa, M., Wilson, E. T. & Wieschaus, E. A putative cell signal encoded by the folded gastrulation gene coordinates cell shape changes during *Drosophila* gastrulation. *Cell* **76,** 1075–1089 (1994).
12. Kiehart, D. P. Molecular genetic dissection of myosin heavy chain function. *Cell* **60,** 347–350 (1990).
13. Karess, R. E. *et al.* The regulatory light chain of nonmuscle myosin is encoded by spaghetti-squash, a gene required for cytokinesis in *Drosophila*. *Cell* **65,** 1177–1189 (1991).
14. Young, P. E., Richman, A. M., Ketchum, A. S. & Kiehart, D. P. Morphogenesis in *Drosophila* requires nonmuscle myosin heavy chain function. *Genes Dev.* **7,** 29–41 (1993).
15. Lecuit, T., Samanta, R. & Wieschaus, E. *slam* encodes a developmental regulator of polarized membrane growth during cleavage of the *Drosophila* embryo. *Dev. Cell* **2,** 425–436 (2002).
16. Stein, J. A., Broihier, H. T., Moore, L. A. & Lehmann, R. Slow as Molasses is required for polarized membrane growth and germ cell migration in *Drosophila*. *Development* **129,** 3925–3934 (2002).
17. Kiehart, D. P., Galbraith, C. G., Edwards, K. A., Rickoll, W. L. & Montague, R. A. Multiple forces contribute to cell sheet morphogenesis for dorsal closure in *Drosophila*. *J. Cell Biol.* **149,** 471–490 (2000).
18. Hutson, M. S. *et al.* Forces for morphogenesis investigated with laser microsurgery and quantitative modeling. *Science* **300,** 145–149 (2003).
19. Wolf, W. A., Chew, T. L. & Chisholm, R. L. Regulation of cytokinesis. *Cell. Mol. Life Sci.* **55,** 108–120 (1999).
20. Glotzer, M. Animal cell cytokinesis. *Annu. Rev. Cell Dev. Biol.* **17,** 351–386 (2001).
21. Jordan, P. & Karess, R. Myosin light chain-activating phosphorylation sites are required for oogenesis in *Drosophila*. *J. Cell Biol.* **139,** 1805–1819 (1997).
22. Wheatley, S., Kulkarni, S. & Karess, R. *Drosophila* nonmuscle myosin II is required for rapid cytoplasmic transport during oogenesis and for axial nuclear migration in early embryos. *Development* **121,** 1937–1946 (1995).
23. Winter, C. G. *et al.* *Drosophila* Rho-associated kinase (Drok) links Frizzled-mediated planar cell polarity signaling to the actin cytoskeleton. *Cell* **105,** 81–91 (2001).
24. Uehata, M. *et al.* Calcium sensitization of smooth muscle mediated by a Rho-associated protein kinase in hypertension. *Nature* **389,** 990–994 (1997).
25. Narumiya, S., Ishizaki, T. & Uehata, M. Use and properties of ROCK-specific inhibitor Y-27632. *Methods Enzymol.* **325,** 273–284 (2000).
26. Royou, A., Sullivan, W. & Karess, R. Cortical recruitment of nonmuscle myosin II in early syncytial *Drosophila* embryos: its role in nuclear axial expansion and its regulation by Cdc2 activity. *J. Cell Biol.* **158,** 127–137 (2002).
27. Johansen, K. A., Iwaki, D. D. & Lengyel, J. A. Localized JAK/STAT signaling is required for oriented cell rearrangement in a tubular epithelium. *Development* **130,** 135–145 (2003).
28. Jazwinska, A., Ribeiro, C. & Affolter, M. Epithelial tube morphogenesis during *Drosophila* tracheal development requires Piopio, a luminal ZP protein. *Nature Cell Biol.* **5,** 895–901 (2003).
29. Tree, D. R., Ma, D. & Axelrod, J. D. A three-tiered mechanism for regulation of planar cell polarity. *Semin. Cell Dev. Biol.* **13,** 217–224 (2002).

Supplementary Information accompanies the paper on **www.nature.com/nature**.

Acknowledgements We thank J. M. Philippe and J. Della Rovere for their technical help; A. Pelissier for the staining shown in Fig. 2c; R. Karess, D. Kiehart and H. Oda for sending key reagents; F. Pilot and C. Henderson for insights; F. Schweisguth for a useful suggestion; and S. Cohen, J. Ewbank, C. Henderson, S. Kerridge, F. Pilot, O. Pourquié and J. Pradel for comments on the manuscript. Research in the Lecuit laboratory is supported by an ATIP grant from the CNRS, by the Fondation pour la Recherche Médicale, the Association pour la Recherche contre le Cancer and the EMBO Young Investigator Programme.

Competing interests statement The authors declare that they have no competing financial interests.

Correspondence and requests for materials should be addressed to T.L. (lecuit@ibdm.univ-mrs.fr).

Structure of a complex between a voltage-gated calcium channel β-subunit and an α-subunit domain

Filip Van Petegem, Kimberly A. Clark, Franck C. Chatelain & Daniel L. Minor Jr

Cardiovascular Research Institute, Departments of Biochemistry and Biophysics, and Cellular and Molecular Pharmacology, University of California San Francisco, 513 Parnassus Avenue, Box 0130, San Francisco, California 94143, USA

Voltage-gated calcium channels (Ca_Vs) govern muscle contraction, hormone and neurotransmitter release, neuronal migration, activation of calcium-dependent signalling cascades, and synaptic input integration[1]. An essential Ca_V intracellular protein, the β-subunit ($Ca_V\beta$)[1,2], binds a conserved domain (the α-interaction domain, AID) between transmembrane domains I

and II of the pore-forming α_1 subunit[3] and profoundly affects multiple channel properties such as voltage-dependent activation[2], inactivation rates[2], G-protein modulation[4], drug sensitivity[5] and cell surface expression[6,7]. Here, we report the high-resolution crystal structures of the $Ca_V\beta_{2a}$ conserved core, alone and in complex with the AID. Previous work suggested that a conserved region, the β-interaction domain (BID), formed the AID-binding site[3,8]; however, this region is largely buried in the $Ca_V\beta$ core and is unavailable for protein–protein interactions. The structure of the AID–$Ca_V\beta_{2a}$ complex shows instead that $Ca_V\beta_{2a}$ engages the AID through an extensive, conserved hydrophobic cleft (named the α-binding pocket, ABP). The ABP–AID interaction positions one end of the $Ca_V\beta$ near the intracellular end of a pore-lining segment, called IS6, that has a critical role in Ca_V inactivation[9,10]. Together, these data suggest that $Ca_V\beta$s influence Ca_V gating by direct modulation of IS6 movement within the channel pore.

The 1.97 Å resolution structure of the $Ca_V\beta_{2a}$ core shows that $Ca_V\beta$s comprise two well-conserved domains (Fig. 1a). The first, an SH3 fold, contains five antiparallel β-strands (β1–β5), a 3_{10} helix (η1), and two α-helices (α1 and α2) that lie amino-terminal to β1 and carboxy-terminal to β4, respectively. The strand that completes the SH3 fold, β5 (residues 217–224), is separated in the primary structure from the core of the SH3 domain by approximately 70 residues (variable domain 2, V2, a site of splice variation and amino acid insertions and deletions[2]) that are absent from the structure (Fig. 1b). The second conserved domain consists of a five-stranded parallel β-sheet (β6–β10), surrounded by six α-helices (α3–α8) and two 3_{10} helices (η2 and η3), and is related to the core of nucleotide kinase enzymes.

$Ca_V\beta$s share structural features with membrane-associated guanylate kinases (MAGUKs), a protein scaffold family that organizes signalling components near membranes[11]. MAGUKs contain one or more PDZ domains N-terminal to an SH3 domain, a bridging region known as a HOOK domain and a nucleotide kinase domain[11,12]. PDZ domains are approximately 100 residues long. The $Ca_V\beta_{2a}$ structure indicates that $Ca_V\beta$s lack N-terminal PDZ domains. There are too few residues N-terminal to the SH3 domain (even in $Ca_V\beta_{1b}$, the $Ca_V\beta$ with the longest (55 amino acids) N-terminal variable region 1, V1) to fold as a PDZ domain. The absence of a PDZ domain distinguishes $Ca_V\beta$s from canonical MAGUK proteins.

Comparison of $Ca_V\beta_{2a}$ with a representative MAGUK, PSD-95 (refs 12, 13), reveals other differences. Superposition of the nucleotide kinase domains shows that the relative orientations of the SH3 and nucleotide kinase domains differ by approximately 90°, an arrangement that makes $Ca_V\beta_{2a}$ a more elongated structure (Fig. 2a). The nucleotide kinase domain of MAGUKs is homologous to guanylate kinases and retains guanosine monophosphate (GMP) binding, but key residues for enzymatic function are missing[12]. The four-stranded β-sheet nucleotide kinase subdomain that binds GMP in MAGUKs is absent in $Ca_v\beta_{2a}$ (Fig. 2a). Furthermore, two $Ca_V\beta_{2a}$ loops (between β7–η2 and β8–β9) occlude part of the binding site for the GMP guanosine ring. Thus, the $Ca_V\beta$ nucleotide kinase domain seems to have lost the ability to bind nucleotides.

The structures of $Ca_v\beta_{2a}$ and PSD-95 SH3 domains are similar (Fig. 2b). Neither is compatible with canonical modes of proline-rich ligand binding. Both lack the aromatic residues necessary for ligand engagement[13], and the surface that would bind polyproline ligands is blocked by the α2 helix[12,13]. In PSD-95, residues C-terminal to the nucleotide kinase domain contribute an extra SH3 β-strand that is absent from canonical SH3 domains[13] and absent in $Ca_v\beta_{2a}$. The HOOK domain, present in MAGUKs and $Ca_V\beta_{2a}$, bridges SH3 β-strands β4 and β5 and comprises α2 and variable domain 2 of $Ca_V\beta_{2a}$. HOOK domains are important regulatory regions for interactions of MAGUKs with other proteins[11,12,14] and may serve a similar function for $Ca_v\beta$ protein–protein interactions.

$Ca_v\beta$s exert their effects on Ca_V function by binding the pore-forming α_1 subunit at a conserved, 18-residue sequence located between membrane domains I and II (the AID)[3,15] (Fig. 3a). Interpretation of mutagenesis and biochemical studies suggested that $Ca_v\beta$–AID interactions occur through a 41-residue segment ($Ca_V\beta_{2a}$ residues 212–252) termed the β-interaction domain (BID)[8,16]. The $Ca_V\beta_{2a}$ structure shows that the central region of the BID, which includes the residues previously thought to be important for BID–AID interactions[8], is entirely buried and cannot participate directly in protein–protein interactions (Fig. 3b). Two putative BID phosphorylation sites[8,16] are also buried in this region. Given the extent of burial, mutations used to determine the relative importance of residues involved in BID–AID interactions (for example, proline to arginine)[8] are likely to have abolished AID binding by disrupting the folded structure of the nucleotide kinase domain rather than by perturbing direct AID contacts. Although it would appear that the $Ca_V\beta_{2a}$ structure conflicts with previous data,

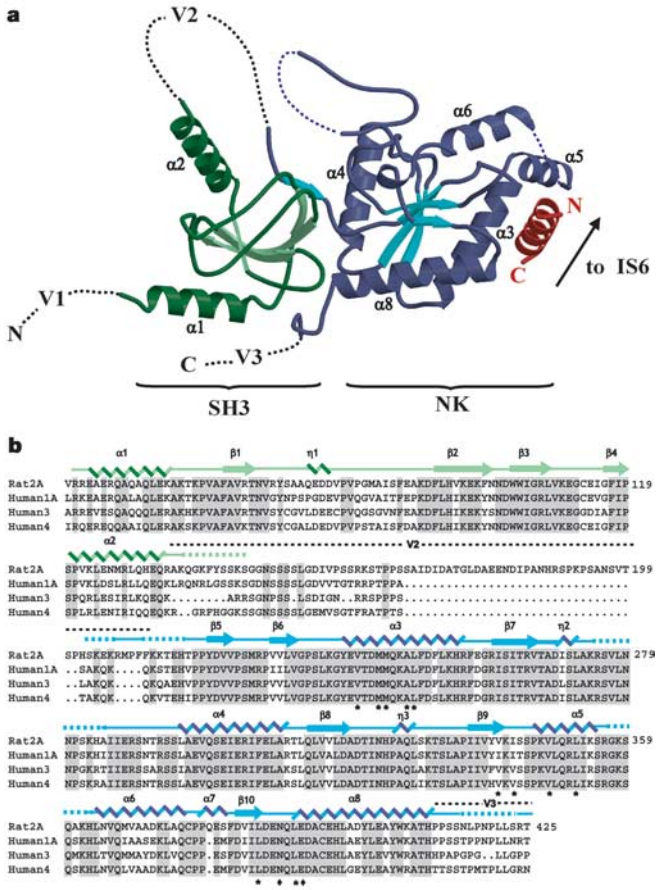

Figure 1 Structure of the $Ca_V\beta_{2a}$–$Ca_V1.2$ AID complex. **a**, Ribbon diagram of the complex. Dashed lines indicate regions absent from the structures. SH3 and nucleotide kinase (NK) domains are shown in green and blue, respectively. The AID is shown in red. $Ca_V\beta_{2a}$ α-helices are labelled. Variable regions V1, V2 and V3 are indicated. The $Ca_V\beta_{2a}$ unbound structure is similar to that shown here for the complex. The arrow indicates where the AID connects to transmembrane segment IS6. **b**, Sequence alignment of representatives of each $Ca_V\beta$ isoform. The top sequence shows residues 40–425 of rat $Ca_v\beta_{2a}$. Numbers on the right denote each line's terminal residue. Shading denotes residues identical among isoforms. The two $Ca_v\beta_{2a}$ domains used for crystallization are indicated in green and blue, respectively. Secondary structure elements are indicated: α, α-helix; η, 3_{10} helix; β, β-strand. Dashed lines indicate residues present in the crystallized constructs but absent in the electron density. Location of the V2 and part of the V3 regions are shown. Asterisks identify residues that contribute side-chain contacts to the AID-binding pocket; diamonds mark side chains with direct hydrogen bonds to the AID.

most of the supporting evidence for the BID–AID interaction relied on indirect functional experiments and direct BID–AID binding was never demonstrated[8,16].

If the BID does not interact directly with the AID, how do $Ca_v\beta_{2a}$ and the AID interact? To answer this, we solved the high-resolution (2.00 Å) structure of a complex between the conserved $Ca_V\beta_{2a}$ core and an 18-residue peptide containing the AID from the L-type channel $Ca_v1.2$. The electron density reveals the first 16 residues of the AID and the location of the binding pocket on $Ca_v\beta_{2a}$ (Fig. 3c). Overall, the $Ca_v\beta_{2a}$ structure is very similar to the unbound form (root-mean-square deviation $(RMSD)_{C\alpha} = 0.397$ Å) and bears only a few conformational changes in side chains near the AID-binding pocket ($Ca_v\beta_{2a}$ residues M244, N390, E393 and R351). The AID forms an α-helix that is anchored to the binding pocket through a set of conserved residues (AID residues L434, G436, Y437, W440 and I441) that are important for $Ca_V\beta$ binding and for α-subunit modulation by $Ca_V\beta$s[8,15,17]. These residues bind a deep groove that we call the α-binding pocket (ABP), formed by helices α3, α5 and α8 of the $Ca_v\beta_{2a}$ nucleotide kinase domain at a site distal to the SH3 domain (Figs 1a, 3b and 4a).

The complex buries approximately 730 $Å^2$ of ABP surface, of which about 350 $Å^2$ are hydrophobic. AID side chains D433, W440 and Q443 make direct hydrogen bonds to the ABP (Supplementary Fig. 1). The depth and extent of burial of the aromatic AID positions Y437 and W440 is particularly striking (Fig. 4b, c). The AID Y437 hydroxyl group is central to a buried hydrogen bond network comprising three water molecules, AID residue D433 and five $Ca_V\beta_{2a}$ residues (Supplementary Fig. 1). Mutation of this tyrosine to phenylalanine greatly diminishes AID–$Ca_V\beta$ binding[15]. The extensive AID–ABP interactions are consistent with biochemical experiments demonstrating strong AID–$Ca_V\beta$ interaction (dissociation constant ~6–20 nM)[18]. The $Ca_V\beta$ side chains that contact the AID are highly conserved among $Ca_V\beta$ isoforms (see Figs 1b, 3a and 4a; see also Supplementary Fig. 1). Thus, both binding partners engage each other through conserved residues to create the AID–ABP interaction.

Interactions between the $Ca_V\alpha_1$ and $Ca_V\beta$ subunits markedly

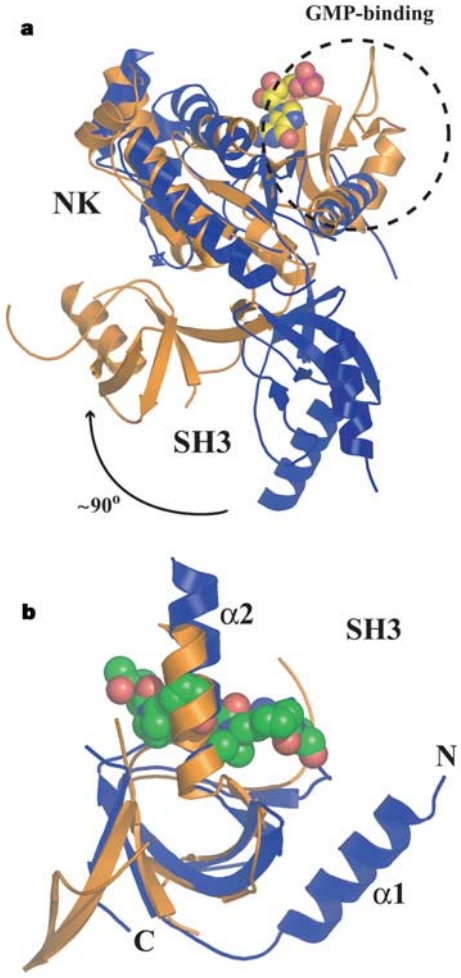

Figure 2 Structural comparisons between PSD-95 (gold) and $Ca_V\beta_{2a}$ (blue). **a**, Superposition of $Ca_V\beta_{2a}$ and PSD-95 nucleotide kinase domains ($RMSD_{C\alpha} = 3.9$ Å). The dashed circle indicates the guanosine-monophosphate (GMP)-binding domain present in PSD-95 but absent in $Ca_V\beta_{2a}$. The guanosine monophosphate molecule bound to PSD-95 is displayed in space-filling representation. Nucleotide kinase (NK) and SH3 domains are indicated. The relative change in SH3 domain orientation is indicated. **b**, Superposition of PSD-95 and $Ca_V\beta_{2a}$ SH3 domains ($RMSD_{C\alpha} = 1.6$ Å). Position of the polyproline ligand from a superposition with the Sem5 SH3 domain (Protein Data Bank code 2SEM) ($RMSD_{C\alpha} = 1.8$ Å) is shown in space-filling representation. The Sem5 SH3 is not shown. The DALI server generated the superpositions (http://www.ebi.ac.uk/dali/).

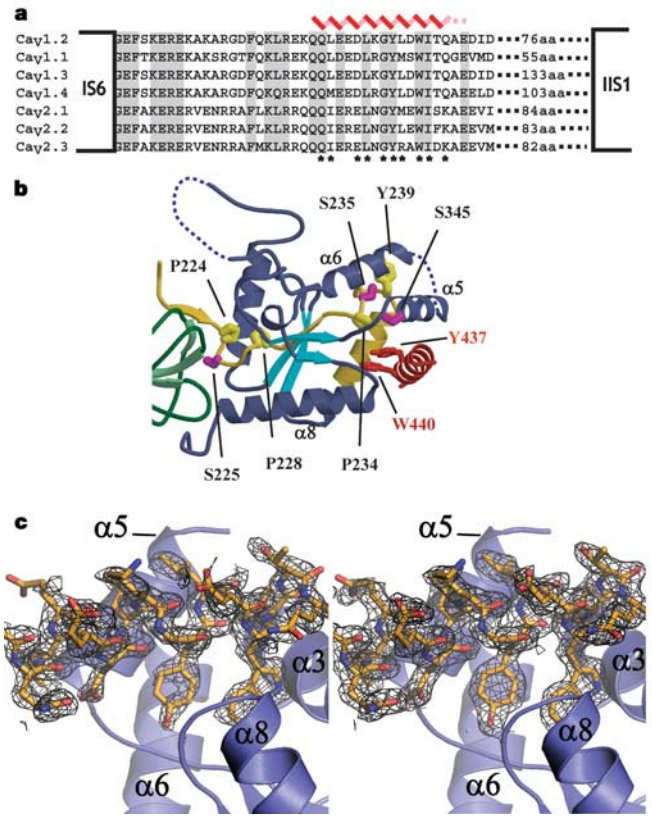

Figure 3 Features of the AID–$Ca_V\beta_{2a}$ interaction and location of the previously described BID. **a**, Sequence alignment of AID domains ($Ca_V1.2$ residues 428–445) and neighbouring residues. The positions of the last transmembrane segment of transmembrane domain I (IS6) and the first transmembrane segment of transmembrane domain II (IIS1) are shown. Secondary structure of the AID from the co-crystal structure is indicated (red). Dashed lines indicate residues absent from the electron density. Asterisks identify side-chain contacts with $Ca_V\beta_{2a}$ closer than 4 Å. **b**, Position of the previously described BID (residues 212–252; yellow)[3,8]. Residues previously proposed to mediate AID–BID interactions (P224, P228, P234, Y239) are indicated and have relative accessibilities of 1.4%, 0%, 0% and 32.4%. Putative PKC sites S225, S235 and S345 are also shown (magenta) and have relative accessibilities of 8.8%, 0% and 35.4%, respectively. S345 accessibility reduces to 12% in the complex. Accessibility values are relative to a tripeptide, Gly-X-Gly. **c**, The left panel shows $F_o - F_c$ electron density, contoured at 2σ, for the AID–$Ca_V\beta_{2a}$ complex before building the AID. The right panel shows final $2F_o - F_c$ density, contoured at 1σ, for the AID from the refined AID–$Ca_V\beta_{2a}$ structure (right). In both panels the final AID model is shown.

influence the cell surface expression of functional channels[6,7]. Control of Ca_V trafficking by regulating $Ca_V\alpha_1$–$Ca_V\beta$ interactions is emerging as an important means of modulating cellular excitability[7]. Ca_V channel subtypes are major clinical targets for drugs that treat cardiovascular disease, migraine and pain[19]. Development of compounds that could interfere with the AID–ABP binding interactions might provide new ways to modulate Ca_V function in pathological states.

The $Ca_V\beta$–AID structure provides a starting point for understanding how $Ca_V\beta$ modulates numerous channel properties. G-protein βγ subunits (Gβγ) inhibit Ca_V function[1,4]; however, the sites of Gβγ–Ca_V interactions and precise inhibitory mechanisms remain highly controversial[4]. Biochemical experiments show that Gβγ binds the Ca_V2 AID and that mutations at AID positions Q1, Q2, R5, L7, G9 and Y10 (corresponding to $Ca_v1.2$ AID residues 428, 429, 432, 434, 436 and 437) abolish Gβγ–AID binding[20]. In contrast, other studies suggest that the *in vitro* Gβγ–AID interaction is functionally irrelevant and that the relevant Gβγ-binding determinants lie elsewhere in the channel cytoplasmic domains[21,22]. The structure of the $Ca_V\beta_{2a}$–AID complex shows that three of the putative Gβγ–AID interacting positions (L7, G9 and Y10), which are invariant in Ca_V1 and Ca_V2 channels (Fig. 3a), are deeply buried by interactions with $Ca_V\beta$ (Fig. 4a, b; see also Supplementary Fig. 2 and Table 2). The extent of burial of these residues, which are critical for maintaining $Ca_V\beta$–AID association[3,15], suggests that Gβγ and $Ca_V\beta$ cannot bind to the AID simultaneously. Taken together with the observation that the Gβγ–AID affinity is at least 10–20-fold weaker than the $Ca_V\beta$–AID[20] affinity, the structure also indicates that it is unlikely that Gβγ could effectively compete with $Ca_V\beta$ for AID binding without drastic structural rearrangement of the $Ca_V\beta$–AID complex. Thus, our data lend support to the view that the major Gβγ interaction sites lie in other Ca_V cytoplasmic domains[21–23].

How might $Ca_V\beta$s affect channel gating? Although the detailed mechanisms of Ca_V inactivation processes remain unknown, functional experiments show that the IS6 pore-lining segment has a key role[10]. Motions of pore-lining transmembrane segments are a common theme emerging in ion channel gating[24,25]. Twenty-two residues separate the AID helix N terminus from the cytoplasmic end of IS6. We do not know the structure, but sequence evaluation suggests that these residues have a high helix propensity and could readily form a continuous helix between the AID helix and the presumed transmembrane helix of IS6 (Fig. 5a). AID residue 5 (E432, here) slows inactivation when negatively charged (as in Ca_V1 channels) and speeds inactivation when positively charged (as in Ca_V2 channels)[26,27]. This residue is exposed on the surface of the AID helix (Fig. 4a) where it would be available to interact with other parts of the channel and could influence the rates of movement of the $Ca_V\beta$–AID complex and therefore IS6. The profound inactivation rate slowing caused by $Ca_V\beta_{2a}$ requires anchoring of the N terminus to the membrane by palmitoylation[28]. Orientation of the AID helix towards IS6 places the N-terminal membrane anchor on the periphery of the α_1 subunit and suggests that $Ca_V\beta_{2a}$ slows channel inactivation by restricting the movement of the IS6 transmembrane domain. $Ca_V\beta$s have a deep groove between the SH3 and

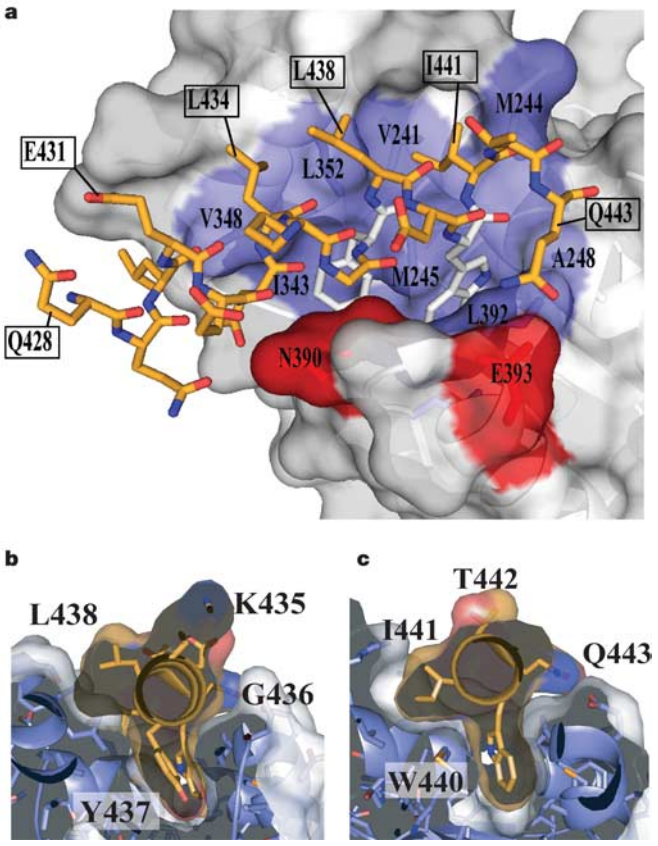

Figure 4 AID–ABP interactions. **a**, Surface representation of the $Ca_V\beta_{2a}$ ABP, bound to the AID. The AID (gold) is shown in stick representation. Y437 and W440 are white. $Ca_V\beta_{2a}$ residues that contribute hydrophobic (blue) and hydrogen bond (red) side-chain contacts to the AID are labelled. Select residues of the AID are labelled to orient the reader. **b**, **c**, Slices through the AID–ABP interaction at AID positions Y437 and W440 (gold). Labels indicate the AID residues.

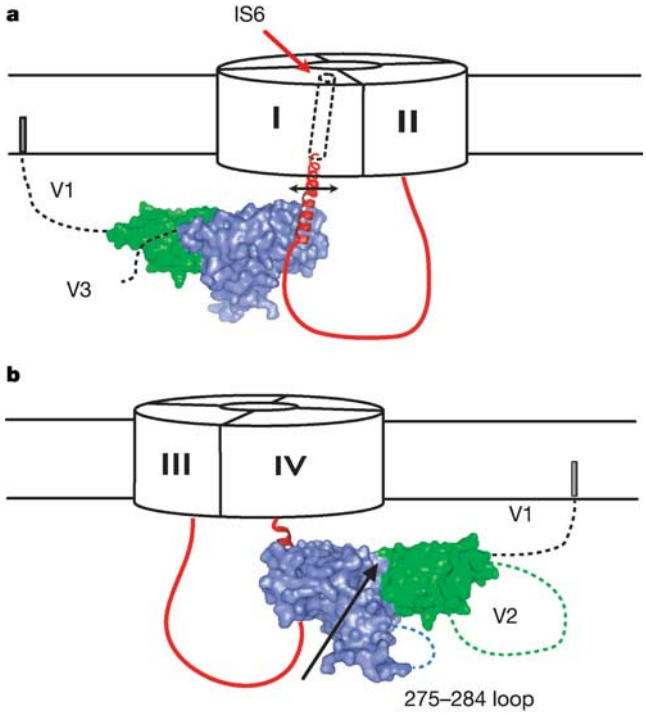

Figure 5 Cartoon of proposed model for how $Ca_V\beta$ affects $Ca_V\alpha_1$ gating. **a**, Orientation of $Ca_V\beta_{2a}$ with respect to the I–II loop (red), pore-forming subunit, and connection to IS6. In $Ca_V\beta_{2a}$, variable region 1 (V1) is tethered to the membrane. The I–II loop between the AID N terminus and IS6 is depicted as a helix. $Ca_V\beta_{2a}$ SH3 and nucleotide kinase domains are coloured green and blue, respectively. The arrow indicates that $Ca_V\beta$ couples to IS6 movements (rotations, translations or both). **b**, View from the opposite side of **a**. The groove between SH3 and nucleotide kinase domains (demarcated by the arrow) and two flexible $Ca_V\beta_{2a}$ regions, the 275–284 loop and variable region 2 (V2), are on the same $Ca_V\beta$ face, opposite the ABP. These regions may interact with other pore-forming subunit cytoplasmic domains.

nucleotide kinase domains that is on the same face as the V2 domain. These features may be used to engage other cytoplasmic parts of the channel[29,30] and allow $Ca_V\beta$ to couple motions in other channel domains directly to IS6 through AID attachment.

The structures presented here represent the first high-resolution view of any part of the voltage-gated calcium channel, and provide an important step towards understanding the detailed molecular mechanism models for how Ca_Vs function. This work strongly suggests that $Ca_V\beta$ affects Ca_V gating properties by directly influencing conformational changes that are likely to occur in the channel pore[10]. □

Methods

The crystal structures of recombinant $Ca_V\beta_{2a}$ and $Ca_V\beta_{2a}$–AID complexes were solved to resolutions of 1.97 Å and 2.00 Å, respectively. The final R/R_{free} values are 18.55%/21.32% for $Ca_V\beta_{2a}$ and 19.97%/24.15% for the $Ca_V\beta_{2a}$–AID complex. Figures were prepared with PyMOL, MOLSCRIPT and RASTER3D. The experimental details for protein expression, purification, crystallization, structure solution, statistics of data collection, phasing and refinement are available as Supplementary Information.

Received 1 March; accepted 23 April 2004; doi:10.1038/nature02588.
Published online 12 May 2004.

1. Catterall, W. A. Structure and regulation of voltage-gated Ca^{2+} channels. *Annu. Rev. Cell Dev. Biol.* **16,** 521–555 (2000).
2. Dolphin, A. C. β-subunits of voltage-gated calcium channels. *J. Bioenerg. Biomembr.* **35,** 599–620 (2003).
3. Pragnell, M. *et al.* Calcium channel β-subunit binds to a conserved motif in the I–II cytoplasmic linker of the α1-subunit. *Nature* **368,** 67–70 (1994).
4. Dolphin, A. C. G protein modulation of voltage-gated calcium channels. *Pharmacol. Rev.* **55,** 607–627 (2003).
5. Hering, S. β-Subunits: fine tuning of Ca^{2+} channel block. *Trends Pharmacol. Sci.* **23,** 509–513 (2002).
6. Bichet, D. *et al.* The I–II loop of the Ca^{2+} channel α1 subunit contains an endoplasmic reticulum retention signal antagonized by the β subunit. *Neuron* **25,** 177–190 (2000).
7. Beguin, P. *et al.* Regulation of Ca^{2+} channel expression at the cell surface by the small G-protein kir/Gem. *Nature* **411,** 701–706 (2001).
8. De Waard, M., Scott, V. E., Pragnell, M. & Campbell, K. P. Identification of critical amino acids involved in α1-β interaction in voltage-dependent Ca^{2+} channels. *FEBS Lett.* **380,** 272–276 (1996).
9. Stotz, S. C., Hamid, J., Spaetgens, R. L., Jarvis, S. E. & Zamponi, G. W. Fast inactivation of voltage-dependent calcium channels. A hinged-lid mechanism? *J. Biol. Chem.* **275,** 24575–24582 (2000).
10. Zhang, J. F., Ellinor, P. T., Aldrich, R. W. & Tsien, R. W. Molecular determinants of voltage-dependent inactivation in calcium channels. *Nature* **372,** 97–100 (1994).
11. Dimitratos, S. D., Woods, D. F., Stathakis, D. G. & Bryant, P. J. Signaling pathways are focused at specialized regions of the plasma membrane by scaffolding proteins of the MAGUK family. *Bioessays* **21,** 912–921 (1999).
12. Tavares, G. A., Panepucci, E. H. & Brunger, A. T. Structural characterization of the intramolecular interaction between the SH3 and guanylate kinase domains of PSD-95. *Mol. Cell* **8,** 1313–1325 (2001).
13. McGee, A. W. *et al.* Structure of the SH3-guanylate kinase module from PSD-95 suggests a mechanism for regulated assembly of MAGUK scaffolding proteins. *Mol. Cell* **8,** 1291–1301 (2001).
14. Paarmann, I., Spangenberg, O., Lavie, A. & Konrad, M. Formation of complexes between Ca^{2+}.calmodulin and the synapse-associated protein SAP97 requires the SH3 domain-guanylate kinase domain-connecting HOOK region. *J. Biol. Chem.* **277,** 40832–40838 (2002).
15. Witcher, D. R., De Waard, M., Liu, H., Pragnell, M. & Campbell, K. P. Association of native Ca^{2+} channel β subunits with the α1 subunit interaction domain. *J. Biol. Chem.* **270,** 18088–18093 (1995).
16. De Waard, M., Pragnell, M. & Campbell, K. P. Ca^{2+} channel regulation by a conserved β subunit domain. *Neuron* **13,** 495–503 (1994).
17. Berrou, L., Klein, H., Bernatchez, G. & Parent, L. A specific tryptophan in the I–II linker is a key determinant of β-subunit binding and modulation in Ca(V)2.3 calcium channels. *Biophys. J.* **83,** 1429–1442 (2002).
18. Opatowsky, Y., Chomsky-Hecht, O., Kang, M. G., Campbell, K. P. & Hirsch, J. A. The voltage-dependent calcium channel β subunit contains two stable interacting domains. *J. Biol. Chem.* **278,** 52323–52332 (2003).
19. Kochegarov, A. A. Pharmacological modulators of voltage-gated calcium channels and their therapeutical application. *Cell Calcium* **33,** 145–162 (2003).
20. De Waard, M. *et al.* Direct binding of G-protein βγ complex to voltage-dependent calcium channels. *Nature* **385,** 446–450 (1997).
21. Zhang, J. F., Ellinor, P. T., Aldrich, R. W. & Tsien, R. W. Multiple structural elements in voltage-dependent Ca^{2+} channels support their inhibition by G proteins. *Neuron* **17,** 991–1003 (1996).
22. Qin, N., Platano, D., Olcese, R., Stefani, E. & Birnbaumer, L. Direct interaction of Gβγ with a C-terminal Gβγ-binding domain of the Ca^{2+} channel α1 subunit is responsible for channel inhibition by G protein-coupled receptors. *Proc. Natl Acad. Sci. USA* **94,** 8866–8871 (1997).
23. Ivanina, T., Blumenstein, Y., Shistik, E., Barzilai, R. & Dascal, N. Modulation of L-type Ca^{2+} channels by Gβγ and calmodulin via interactions with N and C termini of α1C. *J. Biol. Chem.* **275,** 39846–39854 (2000).
24. Miyazawa, A., Fujiyoshi, Y. & Unwin, N. Structure and gating mechanism of the acetylcholine receptor pore. *Nature* **424,** 949–955 (2003).
25. Jiang, Y. *et al.* The open pore conformation of potassium channels. *Nature* **417,** 523–526 (2002).
26. Herlitze, S., Hockerman, G. H., Scheuer, T. & Catterall, W. A. Molecular determinants of inactivation and G protein modulation in the intracellular loop connecting domains I and II of the calcium channel α1A subunit. *Proc. Natl Acad. Sci. USA* **94,** 1512–1516 (1997).
27. Berrou, L., Bernatchez, G. & Parent, L. Molecular determinants of inactivation within the I–II linker of α1E (CaV2.3) calcium channels. *Biophys. J.* **80,** 215–228 (2001).
28. Restituito, S. *et al.* The β2a subunit is a molecular groom for the Ca^{2+} channel inactivation gate. *J. Neurosci.* **20,** 9046–9052 (2000).
29. Walker, D. *et al.* A new β subtype-specific interaction in α1A subunit controls P/Q-type Ca^{2+} channel activation. *J. Biol. Chem.* **274,** 12383–12390 (1999).
30. Walker, D., Bichet, D., Campbell, K. P. & De Waard, M. A β4 isoform-specific interaction site in the carboxyl-terminal region of the voltage-dependent Ca^{2+} channel α1A subunit. *J. Biol. Chem.* **273,** 2361–2367 (1998).

Supplementary Information accompanies the paper on **www.nature.com/nature**.

Acknowledgements We thank J. M. Berger, K. Brejc, D. Fass, D. Julius, E. A. Lumpkin and B. A. Schulman for comments on the manuscript; J. Holton at beamline 8.3.1 at the Advanced Light Source for help with data collection; R. W. Tsien and D. T. Yue for the calcium channel clones; and members of the Minor laboratory for support at all stages of this work. This work was supported by awards to D.L.M. from the McKnight Foundation for Neuroscience, the March of Dimes Basil O'Connor Scholar program, the Alfred P. Sloan Foundation, and the Rita Allen Foundation. D.L.M. is a McKnight Foundation Scholar, an Alfred P. Sloan Research Fellow and a Rita Allen Foundation Scholar.

Competing interests statement The authors declare that they have no competing financial interests.

Correspondence and requests for materials should be addressed to D.L.M. (minor@itsa.ucsf.edu).
Coordinates and structure factors have been deposited in the Protein Data Bank under accession codes 1T0H and 1T0J.

Structural basis of the α_1–β subunit interaction of voltage-gated Ca^{2+} channels

Yu-hang Chen, Ming-hui Li, Yun Zhang, Lin-ling He, Yoichi Yamada, Aileen Fitzmaurice, Yang Shen, Hailong Zhang, Liang Tong & Jian Yang

Department of Biological Sciences, Columbia University, New York, New York 10027, USA

High-voltage-activated Ca^{2+} channels are essential for diverse biological processes. They are composed of four or five subunits, including α_1, α_2-δ, β and γ (ref. 1). Their expression and function are critically dependent on the β-subunit, which transports α_1 to the surface membrane and regulates diverse channel properties[2–4]. It is believed[3–6] that the β-subunit interacts with α_1 primarily through the β-interaction domain (BID), which binds directly to the α-interaction domain (AID) of α_1[7]; however, the molecular mechanism of the α_1–β interaction is largely unclear. Here we report the crystal structures of the conserved core region of β_3, alone and in complex with AID, and of β_4 alone. The structures show that the β-subunit core contains two interacting domains: a Src homology 3 (SH3) domain and a guanylate kinase (GK) domain. The AID binds to a hydrophobic groove in the GK domain through extensive interactions, conferring extremely high affinity between α_1 and β-subunits[4,8]. The BID is essential both for the structural integrity of and for bridging the SH3 and GK domains, but it does not participate directly in binding α_1. The presence of multiple protein-interacting modules in the β-subunit opens a new dimension to its function as a multi-functional protein.

Four different types of β-subunits (β_1–β_4) have been identified, each with multiple splicing variants (for review, see refs 2–4). Previous studies show that the β-subunit contains five regions, with the second and forth being highly conserved (68–92% identity) and the others highly variable among the four β-subfamilies[5,9,10]. The three middle regions form a core that is able to confer most of the functional properties of the full-length β-subunit[5,9]. Molecular modelling indicates that the second and forth regions are homologous to canonical SH3 domains and the yeast GK domain, respectively, and based on this homology, a structural model of